JOURNAL OF GEOPHYSICAL RESEARCH, VOL. 113, C08042, doi:10.1029/2007JC004501, 2008

Boundary wave communication of bottom pressure and overturning changes for the North Atlantic

Vassil M. Roussenov,[1] Richard G. Williams,[1] Chris W. Hughes,[2] and Rory J. Bingham[2]

Received 10 August 2007; revised 24 April 2008; accepted 30 May 2008; published 26 August 2008.

[1] The relationship between changes in sea-surface height, bottom pressure, and overturning is explored using isopycnal model experiments for the North Atlantic. Changes in high-latitude forcing are communicated rapidly over the basin through boundary wave propagation along the continental slope, involving a hybrid mixture of Kelvin and topographic Rossby waves, as well as spreading more slowly through advection along the western boundary. This wave communication leads to coherent signals in sea-surface height and bottom pressure variability extending for several thousand kilometers along the continental slope. The model results are in broad agreement with altimetric diagnostics, and the patterns only alter in detail with the realism of the topography. The adjustment in bottom pressure is directly linked to a change in overturning since west-east contrasts in bottom pressure are associated with a zonal integral in the meridional geostrophic flow. Correlation patterns reveal that temporal changes in overturning are primarily connected to the vertical contrast in bottom pressure, across the shelf and continental slope, along the western boundary.

Citation: Roussenov, V. M., R. G. Williams, C. W. Hughes, and R. J. Bingham (2008), Boundary wave communication of bottom pressure and overturning changes for the North Atlantic, *J. Geophys. Res.*, *113*, C08042, doi:10.1029/2007JC004501.

1. Introduction

[2] Changes in high-latitude forcing induce changes in overturning, which are communicated over the basin through wave propagation and advection along the western boundary. The relative importance of wave propagation and advection in controlling the overturning is not fully established. Using an idealized model without a background circulation, *Johnson and Marshall* [2002] illustrate how overturning changes are communicated through baroclinic Kelvin waves propagating equatorward along the western boundary and eastward along the equator on a time scale of a few months. The variability along the eastern boundary then propagates into the basin interior via baroclinic Rossby waves on a time scale of several years. Their study extends the earlier work of *Kawase* [1987] examining how the abyssal ocean spins up via the propagation of Kelvin waves. While the background circulation might be expected to be important, an idealized model study suggests that the propagation of Kelvin waves is not inhibited by the presence of the Gulf Stream [*Février et al.*, 2007]. While these idealized studies are insightful, they have not included any comparison with observations and our aim is to assess their relevance in a more realistic setting.

[3] Partial support for this view of wave communication is provided by altimetric diagnostics of sea-surface height variability, on periods less than a year, which reveal coherent signals extending over several 1000 km along the continental slope [*Hughes and Meredith*, 2006]. These coherent sea-level changes are interpreted as being due to boundary waves propagating rapidly, effectively along a wave guide, along the continental slope around ocean basins. These boundary waves are a hybrid mixture of baroclinic Kelvin waves and topographic Rossby waves [*Huthnance*, 1978; *Clarke and Van Gorder*, 1994], with typical speeds of 1 ms^{-1} near the equator and 2–3 ms^{-1} at higher latitudes [*Enfield and Allen*, 1980; *Meyers et al.*, 1998]. The boundary waves are defined as baroclinic Kelvin waves for vertical sidewalls with stratification and topographic Rossby waves for sloping sidewalls with no stratification; for discussion of how the different classes of coastally-trapped waves are supported by different combinations of rotation, stratification and sloping topography, see reviews by *Wang and Mooers* [1976], *Mysak* [1980], and *Huthnance et al.* [1986].

[4] The connection between wave communication and the overturning has not been clearly demonstrated in a realistic domain over interannual or longer time scales. While the overturning can locally vary on sub-annual time scales [*Cunningham et al.*, 2007], changes in the overturning are only likely to lead to a significant climate impact on much longer time scales, probably several decades or longer. Thus our interest is in how the boundary wave communication process connects with longer-term changes in the overturning.

[5] In this study, an isopycnal circulation model is used in a realistic setting to assess the connection between the variability of sea-surface, bottom pressure and the over-

[1]Department of Earth and Ocean Sciences, University of Liverpool, Liverpool, UK.
[2]Proudman Oceanography Laboratory, Liverpool, UK.

0148-0227/08/2007JC004501$09.00

turning, extending the idealized model study of *Johnson and Marshall* [2002]. First, the modeled sea-surface height correlations are compared with altimetric diagnostics of *Hughes and Meredith* [2006], second, the adjustment of the bottom pressure field is examined, and finally the connection with changes in the meridional overturning is explored, applying the basin pressure contrasts advocated by *Marotzke et al.* [1999] and *Hirschi and Marotzke* [2007].

2. Model Formulation

[6] The model simulations have been conducted using an isopycnic model (MICOM 2.7 [*Bleck and Smith*, 1990]) with a formulation similar to that employed by *Roussenov et al.* [2006]. The horizontal resolution is either 0.23° or 1.4° on a Mercator grid and 15 σ_2 isopycnal layers in the vertical plus a surface mixed layer with variable density. The model domain extends from 35°S to 65°N and from 98.5°W to 19°E with the topography taken from ETOP05 data averaged within the model grid. At the northern and southern boundaries, sponge layers are incorporated below the mixed layer: isopycnal depths and salinity are relaxed toward climatology in relaxation zones extending for 8° in latitude on the southern boundary and 4° on the northern boundary with the relaxation time scale increasing from 30 days on the boundary to 180 days at the interior edge of the sponge layer. Outside the mixed layer and these sponge layers, the only diapycnal mixing is achieved via a diapycnal mixing coefficient, $\kappa = 10^{-7}/N$, varying with buoyancy frequency N, which typically gives 4×10^{-5} m^2 s^{-1} for $N \sim 2.5 \times 10^{-3}$ s^{-1} within the main thermocline. In addition, the isopycnic model employs isopycnic mixing of tracers and thickness diffusion (using a diffusive velocity of 0.5 cm s^{-1} with Laplacian and biharmonic forms respectively), and deformation-dependent momentum mixing (using a background mixing velocity of 1 cm s^{-1} with a Laplacian dependence).

[7] This model study involves a range of different model experiments (Figure 1a):

[8] 1. The realistic forcing experiment is initialized from Levitus climatology and integrated for 170 years at 0.23° resolution, forced by ECMWF monthly-mean winds and surface fluxes in a repeating climatological mean year (Figure 1a, black line). For the last 20 years, realistic forcing based on the ECMWF reanalysis for the period 1980–2000 is applied, and thus includes interannual variability. Most analyses are based on this period of realistic forcing, referred to as the default integration.

[9] 2. The monthly-mean and realistic forcing experiments are repeated at 1.4° resolution and integrated for 120 years (Figure 1a, gray line).

[10] 3. Annual mean forcing experiments at 0.23° resolution are also integrated for 50 years with any variability being entirely internally generated. This annual mean state is used to initialize 10 year, twin perturbation experiments with a high-latitude, buoyancy perturbation included in one of the experiments. These twin experiments are used to reveal more clearly the time scale of the adjustment process and are separately conducted for realistic and smooth topography (Figure 1a, blue and green lines).

[11] The spin up of the high-resolution model takes longer to reach a statistically-steady state than the coarse-resolution model with a decrease in kinetic energy after 50 years, reflecting the longer time for the eddy velocity and density fields to achieve a mutual equilibrium (Figure 1a). Despite the model integrations being initially forced without any interannual variability, there is long-term internal variability in the kinetic energy with periods of typically 15 years when there is monthly forcing and typically 7 years in the annual mean forcing cases (Figure 1a). Similar long-term variability does not occur in the coarse-resolution 1.4° case, suggesting that the long-term variability is associated with fine-scale dynamics linked with narrower boundary currents or eddy activity. The meridional overturning stream function reaches a maximum of typically 18 Sv with longer term variations of ±4 Sv with high-frequency variations removed by applying a 12-month running mean (Figures 1b and 1c). This temporal variability of the overturning stream function has a different character north and south of the inter-gyre boundary at 40°N (Figure 1c), as explored further by *Bingham et al.* [2007].

3. Sea-Surface Height and Bottom Pressure Variability

3.1. Correlation Patterns From Altimetry and Model Diagnostics

[12] *Hughes and Meredith* [2006] demonstrate how there are coherent sea-level fluctuations running along the continental slope over the globe. Their sea level diagnostics are based upon a combined altimeter TOPEX/Poseidon and ERS-1/2 product [*Ducet et al.*, 2000], with a high-pass filter applied, retaining periods less than one year and with annual and semi-annual cycles removed. Their diagnostics reveal a pattern of high, positive correlation between the subsurface pressure west of Scotland (averaged along a 1000 m depth isobath between 52°N to 63.7°N) and the subsurface pressure extending for several 1000 km along the continental slope of the Northeast Atlantic, as well as along the western and eastern boundaries (Figure 2a, left). This correlation pattern is retained when the altimetric data is smoothed horizontally over a 5° grid and also reveals a negative correlation over the central part of the basin (Figure 2a, right). This large scale, coherent pattern is interpreted in terms of the rapid propagation of boundary waves, a hybrid mixture of baroclinic Kelvin and topographic Rossby waves, along the continental slope around the basin.

[13] The correlation of sea level is now investigated in the realistic model integration (0.23° resolution, ECMWF forcing from 1980–2000) using diagnostics with the annual cycle removed, a high-pass filter applied, and correlated with the same region west of Scotland. Again, there is a coherent, large-scale, positive correlation pattern extending around the North Atlantic (Figure 2b, left). This positive correlation runs along the continental slope of the northern rim and western boundary of the subpolar gyre to 40°N, as well as along the eastern boundary and west of the African coast (10–30°N). Thus an enhanced sea-surface height along the boundaries is correlated with a depressed sea-surface height over the central part of the subtropical gyre, reflecting the implied redistribution of mass within the basin. The correlation patterns only differ in detail when repeated for a coarse resolution (1.4°) (Figure 2b, right): the

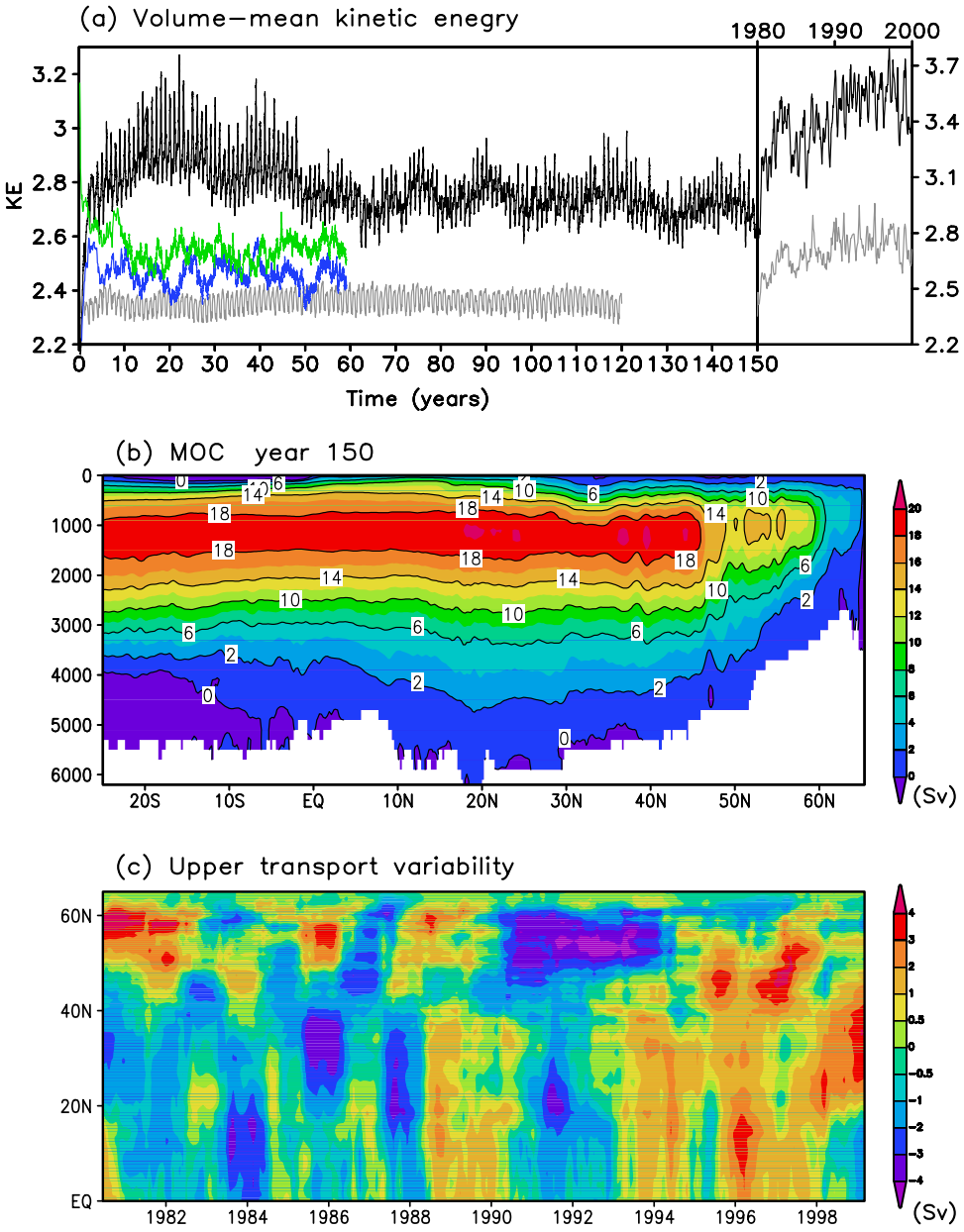

Figure 1. (a) Volume mean kinetic energy for the full set of model experiments: monthly ECMWF forcing at 0.23° (black line), annual forcing at 0.23° with either realistic topography (blue line) or smooth topography (green line), and monthly forcing at 1.4° (gray line). Right: realistic forcing with interannual variability over the last 20 years. (b) Annual mean overturning stream function (Sv) (year 150 in the 0.23° model with monthly forcing). (c) Transport variability (Sv) over the upper 1100 m versus latitude in the 0.23° model over the period forced by 1980–2000 ECMWF reanalysis wind stress and surfaces fluxes (with 12-month running means).

positive correlation extends further south in the coarser model to 28°N off Florida, suggesting that either the finer-scale dynamics or topography is acting to mask or attenuate the propagating sea-surface height anomalies.

[14] The variability in modeled bottom pressure shows a broadly similar correlation pattern to that of the sea-surface height (Figure 2c), reflecting how elevated sea surface increases the underlying bottom pressure in unstratified waters. Again, there is a positive correlation pattern extending along the continental slope running along the northern rim and western side of the subpolar gyre, as well as along the eastern boundary. In this case, the positive correlation along the western boundary extends more clearly further south along the continental slope to around 25°N irrespective of model resolution.

[15] The similarity in the bottom pressure and sea-surface height correlation patterns is to be expected where there is weak stratification. The sea-surface height and bottom pressure anomalies are the same on the shelf and along the upper part of the continental slope. However, in deeper

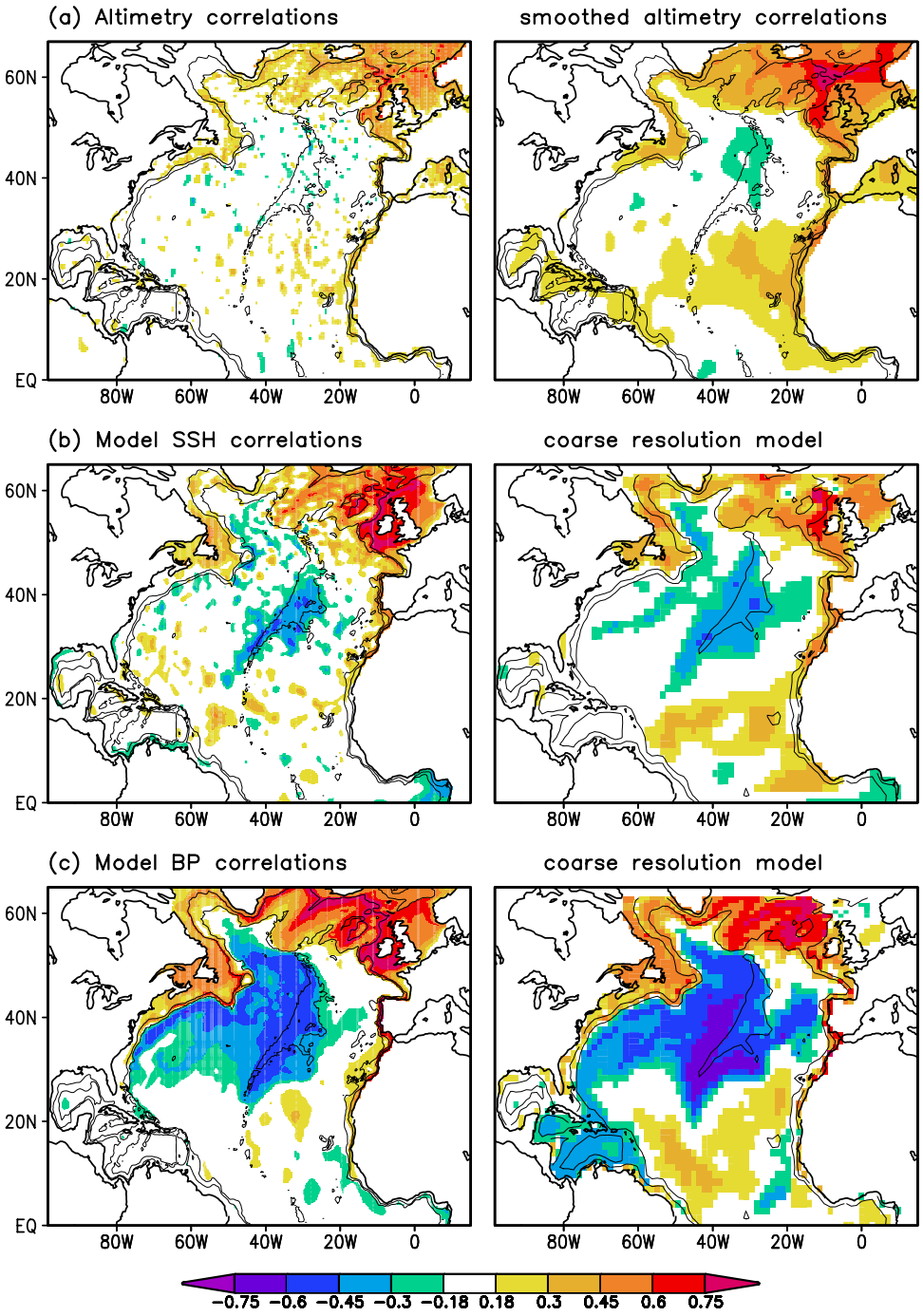

Figure 2. (a) Observational diagnostics showing the correlation of the sub-surface pressure derived from altimetry and averaged along 1000 m isobath west of Scotland with the sub-surface pressure at each grid point. Left: updated from Figure 7 of *Hughes and Meredith* [2006]; right: using a horizontally smoothed altimetry (5° × 5°). Model diagnostics showing similar correlation maps for (b) sea-surface height (SSH) and (c) bottom pressure (BP) for 0.23° and 1.4° resolution (left and right, respectively). All the correlation maps are calculated by comparing the value at each grid point with the value west of Scotland (averaged along 1000 m isobath between 52°N and 63.7°N), with a high-pass filter retaining periods less than 1 year applied; isobaths are included for 1000 and 3000 m (black lines).

waters, the baroclinic compensation leads to the sea-surface height and bottom pressure anomalies being of different sign, reflecting how the flow changes with depth across the main thermocline.

[16] These diagnostics clearly demonstrate that the model is capable of reproducing the coherent boundary signals seen in the altimetric diagnostics (Figure 2a). The model is

now used to explore how these patterns are controlled and how they relate to changes in the meridional overturning.

3.2. How do the Bottom Pressure Signals Evolve?

[17] In order to understand how the sea-surface height and bottom pressure signals evolve, twin experiments are performed, where additional buoyancy forcing is applied over the Labrador Sea. The buoyancy forcing is applied by displacing the deep interface (depth of approximately 1500 m at 60°N), raised 50 m over 5 days over the northern relaxation zone, and then maintained at this new position. To avoid the differences in the twin experiments being masked by externally-driven variability, the experiments are integrated with constant annual mean forcing (without a seasonal cycle) for 10 years after an initial spin up of 50 years.

[18] The sea-surface height anomaly, disturbed minus reference, adjusts rapidly along the western boundary (Figure 3a, left). After 1 month, the negative sea-surface height anomaly extends over the shelf and the upper part of the continental slope along the western boundary, from Labrador to 25°N, with a positive anomaly elsewhere. After 4 months, the negative anomaly extends further south around the Gulf of Mexico and has crossed to the eastern boundary from typically 10°N to 40°N (Figure 3b, left). This pattern is broadly in accord with the adjustment process described by *Johnson and Marshall* [2002] where baroclinic Kelvin waves propagate equatorward from a high-latitude source along the western boundary, cross the equator and generate baroclinic Rossby waves that spread westward into the basin interior. In addition to the boundary-trapped waves, there are large-scale barotropic anomalies on the scale of the barotropic deformation radius, as well as more eddy-scale variability over the extension of the Gulf Stream. After 24 months, any propagating signals are more difficult to detect and the strongest sea-surface height variations are concentrated over the Gulf Stream and its extension (Figure 3c, left), associated with perturbations in the eddy field.

[19] The accompanying bottom pressure anomaly again shows a very similar, large-scale pattern to that of sea-surface height along the boundary (Figure 3a, right), emphasizing how both variables are directly connected and adjust in the same manner through wave communication along the shelf and continental slope. The only important difference is that the bottom pressure anomaly pattern shows less fine-scale variability over the extension of the Gulf Stream and inter-gyre boundary.

[20] For the bottom pressure, an anomaly of opposing sign is formed over the Gulf Stream separation region (Figures 3b and 3c, right). This signal is consistent with the Kelvin wave study of *Février et al.* [2007], where a negative thickness anomaly is formed in the vicinity of the Gulf Stream separation region; the circulation anomaly linked to the Kelvin wave forms a corresponding thickness anomaly as a consequence of potential vorticity conservation.

[21] The communication process is now revealed by mapping the time for the perturbed bottom pressure field to adjust to an initial perturbation of 1 mB in the Labrador Sea. Any circulation anomaly propagating equatorward has a decreasing amplitude in pressure because of compensation for the change in the Coriolis parameter. Consequently, our criterion is defined in terms of the time taken for the absolute value of the bottom-pressure perturbation to adjust to a value of $0.1 + 1.0|\sin\theta|$ in mB where θ is the latitude. For the default twin experiment (Figure 4a), the bottom pressure anomaly adjusts in less than 6 months over the continental slope along the northern and western boundaries of the basin to the equator, and then propagates along the equator to the eastern boundary in less than 1 year. In the interior, there is a band of enhanced interior communication between 10°N and 30°N over several years, which reflects the westward propagation of baroclinic Rossby waves originating from the eastern boundary [*Anderson and Gill*, 1975; *Anderson and Killworth*, 1977].

[22] In order to assess the effect of the detailed topography, the twin experiments are now repeated with smooth topography at the same resolution and at a coarse resolution of 1.4°. For the smooth topography case (Figure 4b), there is a much more rapid communication of the bottom pressure anomaly southward around the western boundary, across the equator and northward along the eastern boundary of the North Atlantic in typically 6 months or less. The interior of the basin has adjusted to the perturbation in less than 5 years. Thus the fine-scale topography in the default integration is acting to inhibit the wave communication, probably through scattering.

[23] Finally, for a model with coarse resolution (Figure 4c), there is still a similar communication along the western boundary and along the equator, but there is less communication in the basin interior, particularly over the subpolar gyre and the central part of the subtropical gyre, and less transfer across the equator into the South Atlantic.

[24] In summary, the region of most rapid adjustment follows the pathways of waves as suggested by the idealized model study of *Johnson and Marshall* [2002]: the waves spread south from a northern source along the western boundary, east along the equator and north along the eastern boundary. Small-scale topography or coarse resolution leads to a weakening of the wave signal, perhaps because of scattering or dissipation of the topographic waves. However, the presence of boundary currents, eddy variability and fine-scale topography does not fundamentally alter the wave communication mechanism, although the anomalies might become harder to detect.

[25] An interesting difference though with *Johnson and Marshall* [2002] is the rapid western boundary adjustment in the southern hemisphere (Figures 4a and 4b), which is not permitted in the idealized study incorporating only baroclinic Kelvin waves. Detailed snapshots of the sea-surface height anomaly over the first year (Figure 3) reveal variability emerging south of 20°S along the western boundary. This cross-equator transfer must be interpreted carefully as there might be an influence of the southern sponge layer. In our view, the signal though is formed through a rapid barotropic communication from the northern source over the entire basin: propagation of barotropic Rossby waves across the basin generates a western boundary current response in the southern basin, well before the arrival of any baroclinic Rossby waves from the northern source, which in turn eventually generates baroclinic boundary waves propagating northward toward the equator. In accord with this view, a coupled atmosphere-ocean model study reveals a rapid communication from the Southern Ocean to

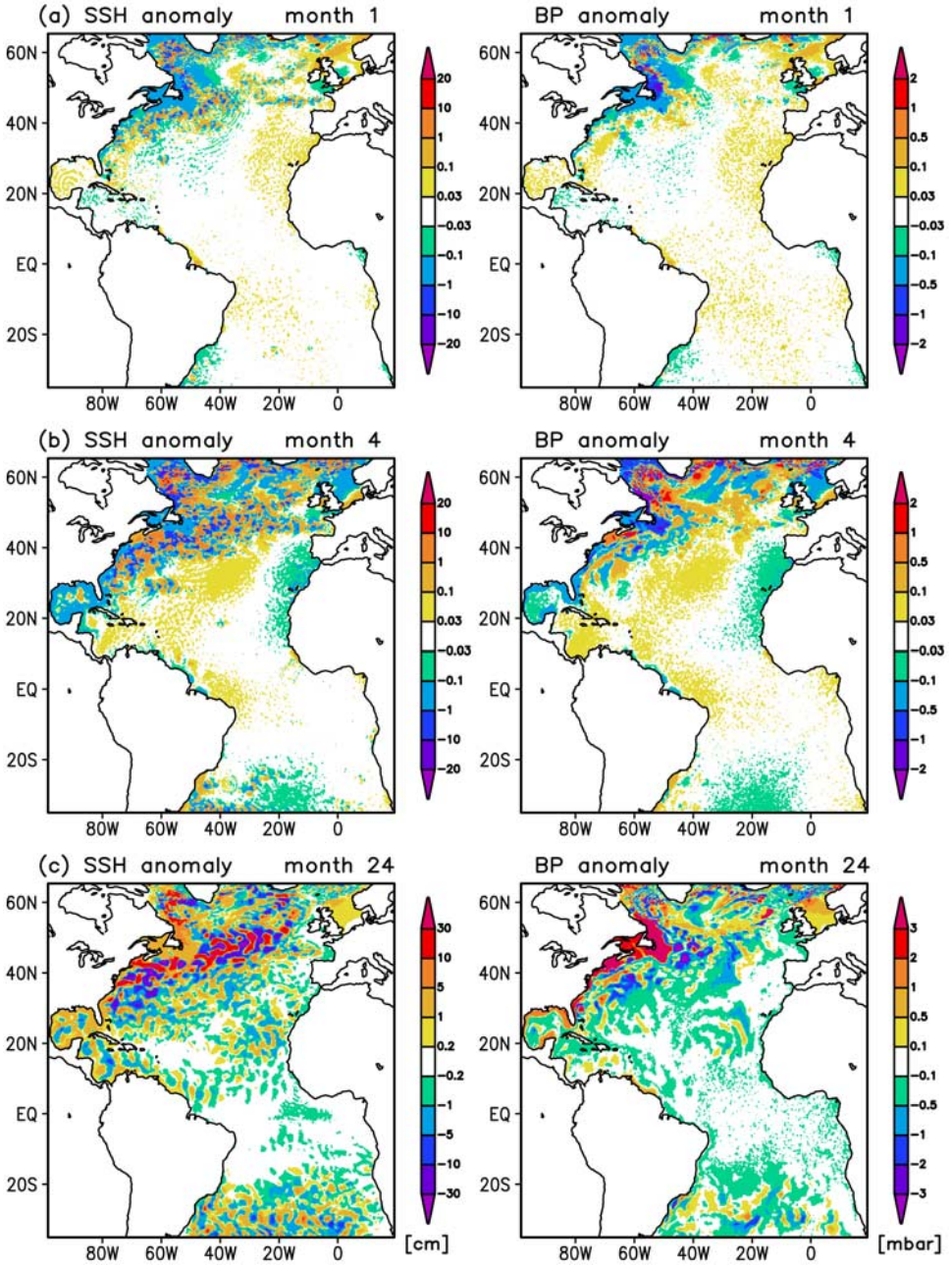

Figure 3. Snapshots of (left) sea-surface height and (right) bottom pressure anomalies from the twin experiment with annual mean forcing. An initial buoyancy forcing perturbation is introduced over the northern relaxation zone, and the anomaly is defined as the model difference between the perturbed and unperturbed states. The anomalies are shown after (a) 1 month, (b) 4 months, and (c) 2 years.

the tropics relying on the propagation of ocean barotropic and baroclinic waves [*Blaker et al.*, 2006].

4. Link Between Overturning and Bottom Pressure Variability

[26] Given the rapid wave adjustment occurring over the basin in the numerical model experiments, consistent with the independent altimetric diagnostics, the larger-scale connection with the meridional overturning is now explored. Firstly, the basin-scale correlation patterns between bottom pressure and the time series for the overturning are examined and, secondly, the link between overturning and the transport inferred from a vertical integral in bottom pressure anomaly is assessed along a zonal section.

4.1. Basin-Scale Correlation Patterns in Overturning and Bottom Pressure

[27] The time-series for the upper ocean transport (Figure 1c) spatially averaged over the northern part of the basin (35°N to 60°N) is now correlated with the variability in bottom pressure for the different model cases, either for the last 20 years or the period 1980 to 2000. Maps of the correlation

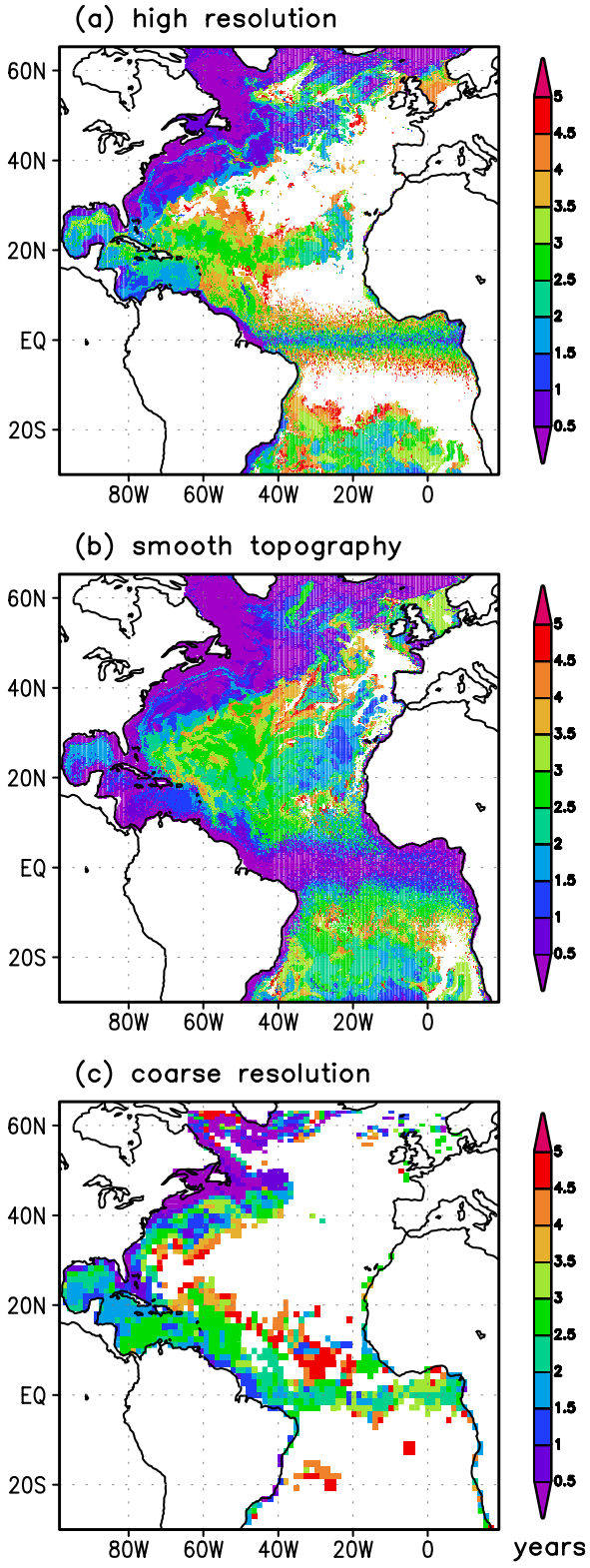

Figure 4. Time of adjustment (years) for the twin experiments with annual mean forcing: time to reach a predefined (Coriolis parameter scaled) difference in the bottom pressure: (a) 0.23° default experiment, (b) 0.23° experiment with smoothed topography, and (c) 1.4° coarse experiment.

pattern are separated into those with time scales shorter or longer than an annual period.

[28] For periods shorter than a year retained (Figure 5a, left), there is a negative correlation along the shelf together with a narrow, positive correlation along the continental slope, between depths of 1000 m and 3000 m, from the northern boundary to 20°N on both the western and eastern boundaries. In the interior, there is also a negative correlation over the deep interior of the western basin. This coherent boundary signal along the continental slope is very similar to the high-frequency, sea-surface height correlation pattern, seen in both the altimetric data and the model (Figure 2). At high frequencies, this boundary pattern is also seen when smooth topography is used, extending southward of 45°N along the western boundary to the equator, but becomes smeared out when a coarse resolution is adopted and the shelf is not fully resolved (Figures 5b and 5c).

[29] These high-frequency, correlation patterns for the overturning are of interest in directly relating to the high-frequency, altimetric diagnostics, supporting the view that the same wave processes are acting to communicate sea-surface height and overturning changes. However, overturning changes only become important for the climate system on periods much longer than a few years because of their importance in transporting heat, while other processes, such as the seasonal heat storage and wind-induced changes of the thermocline dominate on shorter time scales.

[30] For periods longer than one year retained, an increase in overturning is again correlated along the western boundary with a decrease in bottom-pressure along the shelf and, conversely, an increase in bottom-pressure along the continental slope at depths between 1000 m and 3000 m (Figure 5a, right). This coherent pattern of opposing signals on the shelf and continental slope is more clearly revealed in the model experiment with smoothed topography (Figure 5b), which suggests again how fine-scale topography acts to attenuate the wave communication process. This correlation pattern, not surprisingly, becomes less clear and smeared out in the coarse resolution case (Figure 5c).

[31] The connection between the bottom pressure and the overturning is now explored more formally and evaluated in the model for a zonal section along 36°N.

4.2. Zonal Integral of Geostrophic Balance

[32] In order to understand the connection with the overturning, following *Marotzke et al.* [1999] and *Baehr et al.* [2004], consider the definition for the geostrophic meridional velocity,

$$\rho_o f v_g = \frac{\partial P}{\partial x}. \tag{1}$$

Applying a zonal integral from the eastern to western boundaries at a fixed depth, reveals that the integrated geostrophic flow across the basin is the same as the east-west contrast in pressure at the boundaries,

$$\rho_o f \int_{x_w}^{x_e} v_g dx = P_e - P_w, \tag{2}$$

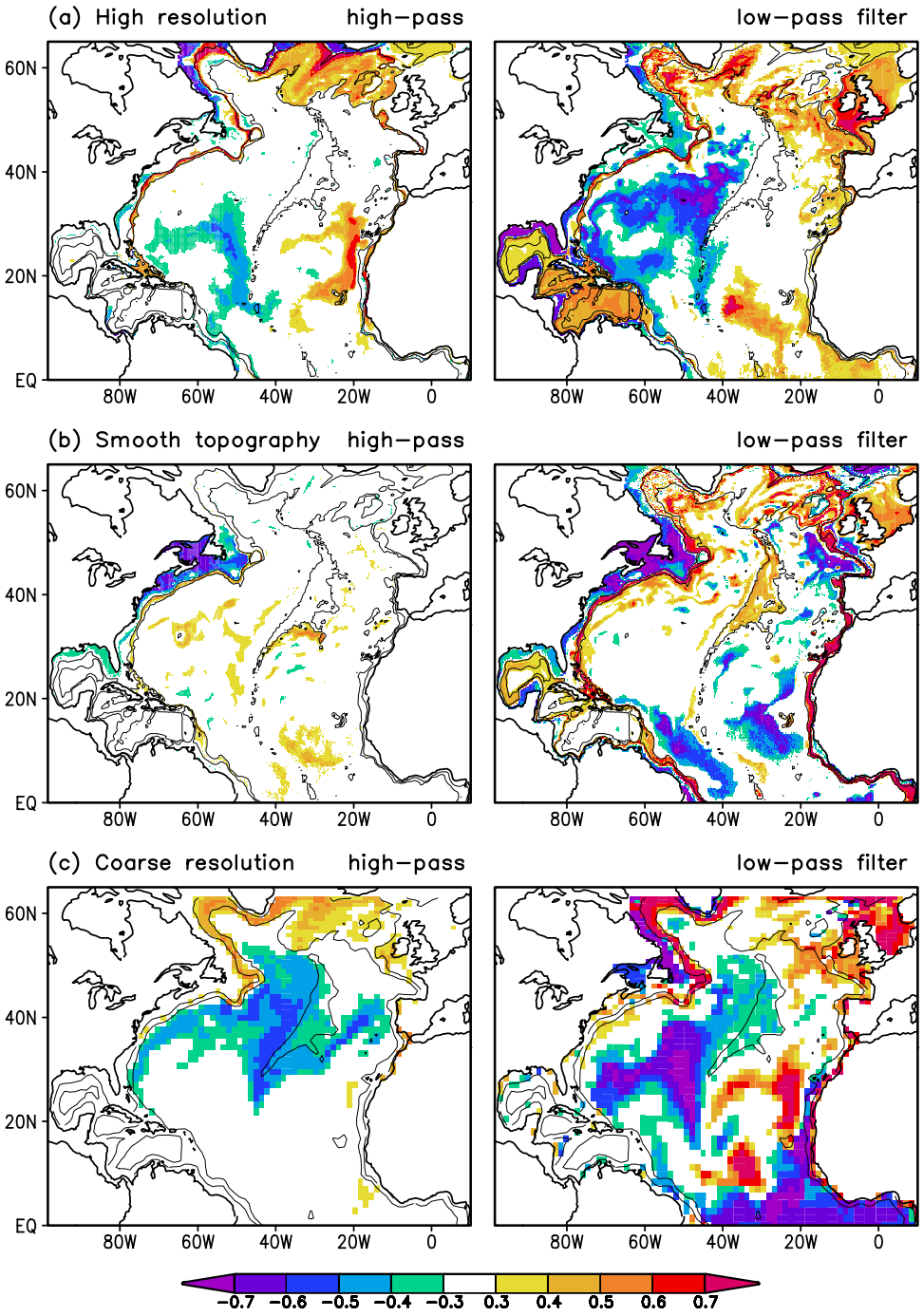

Figure 5. Correlations between bottom pressure and a time series for the meridional overturning, defined by the integrated transport over the upper 1100 m, averaged over the northern latitude range of 35°N to 60°N: (a) 0.23° model with realistic forcing, (b) 0.23° model with annual mean forcing and smooth topography, and (c) 1.4° model with realistic forcing. All correlations have been calculated for a period of 20 years: 1980–2000 in Figures 5a and c and the last 20 model years in Figure 5b. Left: High-pass filtering is applied with periods shorter than 1 year retained; right: Low-pass filtering with periods longer than 1 year retained. Isobaths of 1000 and 3000 m are included as thin black contours.

where the subscripts e and w denote the eastern and western boundaries. The pressures on the boundary, P_e and P_w, are by definition the same as the bottom pressure. Applying a depth integral to (2) from the sea surface η to a fixed depth z gives

$$\rho_o f \int_z^\eta \int_{x_w}^{x_e} v_g dx dz = \int_z^\eta (P_e - P_w) dz, \qquad (3)$$

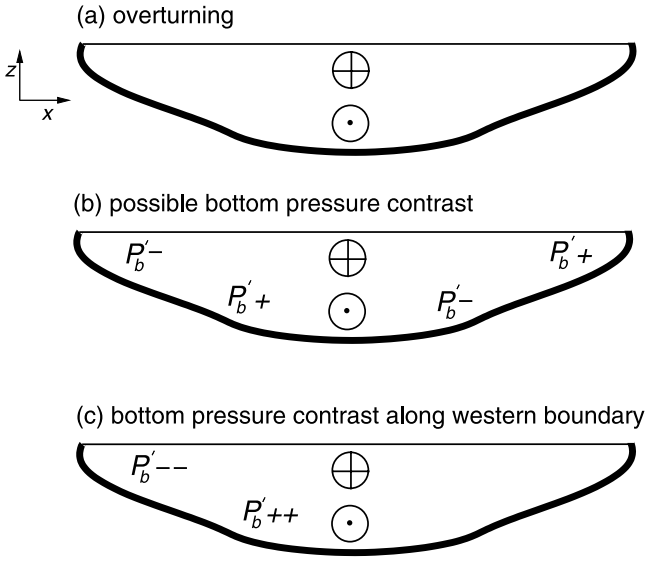

Figure 6. A schematic figure of the west-east bottom pressure contrasts and their link to the overturning for an idealized basin: (a) direction of the overturning stream function with poleward upper flow and equatorward deep flow; (b) accompanying bottom pressure anomalies, P_b', with the bottom pressure less on the western boundary compared with the eastern boundary at shallow depths and reversing to a larger bottom pressure on the western boundary at deeper depths where the overturning has reversed; (c) the bottom pressure contrasts become concentrated on the western boundary (because of the westward propagation of energy from long wavelength, baroclinic Rossby waves).

which can be written in terms of a stream function $\psi(y, z)$ for the meridional geostrophic flow

$$\psi(y,z) = \frac{1}{\rho_o f}\int_z^\eta (P_e - P_w)dz. \tag{4}$$

Thus the overturning stream function for the geostrophic flow can be diagnosed from the depth integral of the west-east contrast in bottom pressure.

[33] For the North Atlantic basin, the overturning involves a poleward surface transport and an equatorward deep transport (Figure 6a), which changes in direction at a depth of typically 1100 m in this model (Figure 1b). Accordingly, one expects that the poleward upper limb of the overturning is associated with the bottom pressure being less on the western boundary than on the eastern boundary, while the equatorward lower limb is associated with the opposing pressure contrast (Figure 6b). In practice, changes in these pressure contrasts are expected to be concentrated along the western boundary (Figure 6c), because of how energy propagates westward in long wavelength, baroclinic Rossby waves.

[34] The previous correlation patterns between the overturning time series and bottom pressure (Figure 5b) indeed reveal how an increase in overturning is associated with a reduction in bottom pressure along the shelf, but at the same time an increase in bottom pressure along the deeper parts of the continental slope on the western boundary.

4.3. Model Diagnostics of Transport Change Inferred From Bottom Pressure

[35] The variability of the meridional overturning (Figure 1c) is now assessed in terms of its connection with the west-east contrasts in bottom pressure, exploiting the integral relationship (4). For this assessment, the high-resolution, default integration is repeated, but now integrated with realistic, interannual ECMWF forcing from 1957 to 2000; these model results for the last 20 years are very similar to the same overlapping period for the previous default integration with realistic forcing for 1980 to 2000.

[36] At 36°N, there are upper ocean meridional transport fluctuations of 6 Sv (evaluated from 100 m to 1100 m) and a general increase in transport for the period from 1985 to 1993 (Figure 7a). At the same time, there are bottom pressure anomalies along the continental slope with a larger amplitude of typically 10 mB at 500 m compared with 5 mB at 3600 m (Figures 7b and 7c). There are generally opposing trends in the bottom pressure at the upper and lower depths along the continental slope. An increase in meridional transport is generally associated with the bottom pressure anomaly becoming more negative along the upper part of the continental slope, but more positive along the deeper part of the continental slope on the western boundary. The variability of the west-east contrast in bottom pressure are dominated by the changes along the western boundary, rather than the eastern boundary (Figures 7b and 7c, full and dashed lines).

[37] The overturning relationship with the integral bottom pressure contrast (4) is now assessed. The overturning

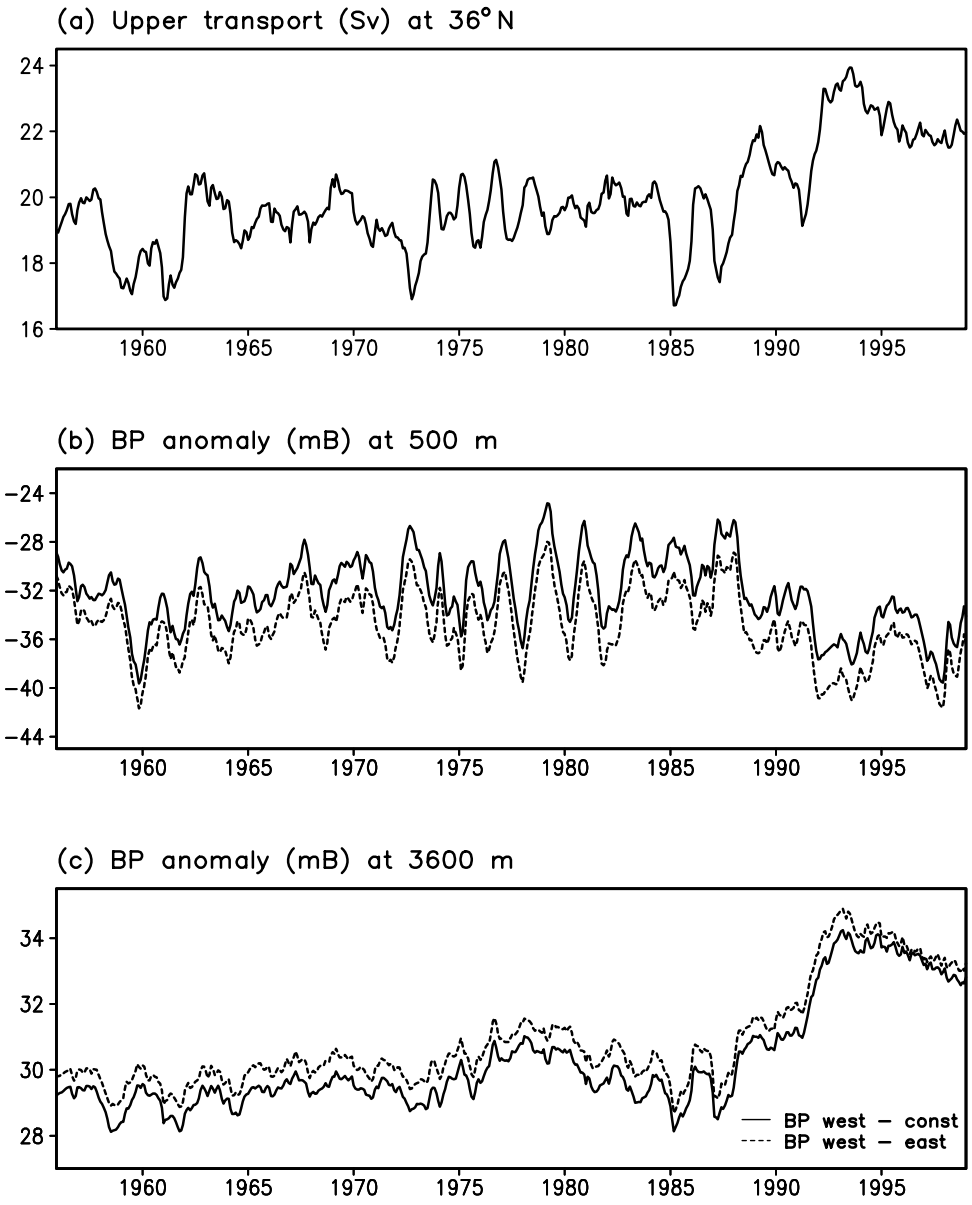

Figure 7. Modeled time series along 36°N with 12-month running means from 1957 to 2000 of (a) vertically integrated upper transport (Sv), from 100 to 1100 m, compared with the bottom pressure anomaly (mB) at a depth of (b) 500 and (c) 3600 m. The bottom pressure anomaly is either taken as the bottom pressure on the western boundary minus the eastern boundary (dashed line) or the bottom pressure on the western boundary minus a constant offset (full line). Note how when the upper transport increases, the bottom pressure anomaly becomes more negative in the upper waters but becomes more positive in the deep waters. This relationship is consistent with the sign of the bottom pressure anomaly indicated in Figure 6.

stream function for changes in the geostrophic flow is estimated by depth integrating the west-east changes in the bottom pressure along the continental slope from 100 m (in order to exclude the Ekman layer) to 1100 m (where the overturning stream function becomes a maximum) and applying a 12-month running mean.

[38] On time scales of 2–3 years, there are differences in the overturning directly measured in the model and that diagnosed from the bottom pressure contrasts (Figure 8) with either an offset in the transport estimate or an enhanced estimate from the bottom pressure (such as from 1977 to 1982). This mismatch probably reflects how the modeled flow is not entirely geostrophic through frictional and temporal changes occurring. However, on a longer time scale, the bottom-pressure derived estimate of the transport is in close agreement with that directly measured in the model (Figure 8). The best agreement is during the period of long-term increase in transport, such as from 1985 to 1993. Over the whole period (1957–2000), the correlation coefficient based on 12-month running means is 0.81 when comparing the actual transport from 100 to 1100 m with the geostrophic transport anomaly derived from the west-east

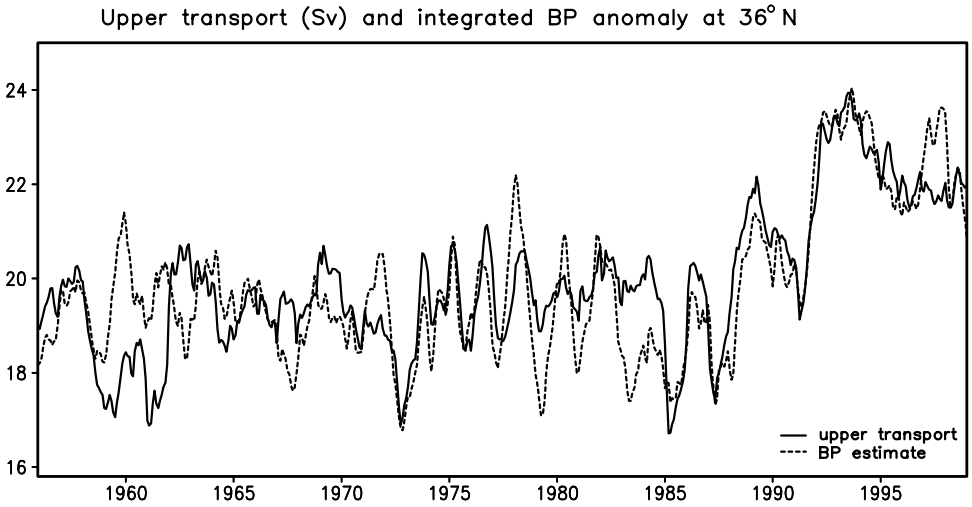

Figure 8. Time series of vertically integrated upper transport (Sv), from 100 to 1100 m, evaluated along 36°N: measured directly in the model (solid line) and diagnosed from the vertical integral of the west-east bottom pressure contrast (dashed line) for the same depth range using (4). The time series is based on 12-month running means from 1957 to 2000.

bottom pressure contrast, and reducing only slightly to 0.79 when using only the western bottom pressure (ignoring the small variations in bottom pressure along the eastern boundary). Including the surface Ekman layer and the Ekman transport contribution does not significantly alter the agreement between the model transport and that inferred from the depth-integral of the bottom pressure contrast (with the Ekman transport term included); the correlation coefficients reduce only slightly to 0.79 and 0.77 between the model transport and that inferred from the west-east bottom pressure contrast and from the western bottom pressure alone.

[39] These model diagnostics broadly support the methodology behind observational studies attempting to monitor long-term changes in the overturning from bottom pressure contrasts along the western boundary. In comparison, *Bingham and Hughes* [2008] describe this calculation in more detail in the context of a Cartesian model, in which stronger correlations are found, and *Hirschi and Marotzke* [2007] give related diagnostics focusing on boundary density in a Cartesian model. The slightly weaker correlations obtained in our study probably reflect slight inaccuracies in using an isopycnal model to evaluate a depth-based diagnostic.

5. Conclusions

[40] The role of boundary waves in communicating high-latitude overturning changes is explored here, as first proposed by *Kawase* [1987] and more recently advocated by *Johnson and Marshall* [2002]. Support for this wave communication is indirectly provided by high-frequency, altimetric diagnostics revealing coherent, sea-surface height signals running along the continental slope [*Hughes and Meredith*, 2006]. Isopycnic model experiments in a realistic Atlantic domain are used here to explore the connection between high-frequency, sea-surface height variability and accompanying bottom pressure signals, and the lower-frequency changes in overturning. Model diagnostics confirm that the sea-surface height variability is rapidly communicated along the continental slope on a time scale of a few months to a year and is associated with similar coherent signals in bottom pressure along the continental slope. The boundary waves providing this rapid communication are a hybrid mixture of baroclinic Kelvin waves and topographic Rossby waves [*Huthnance*, 1978]. The variability in bottom pressure is much larger in amplitude and has longer periods along the western boundary, compared with the eastern boundary. Accordingly, the west-east contrast in bottom pressure are directly linked to the meridional geostrophic velocity across the basin and, thus, the depth-integral of the bottom pressure contrast is linked to the meridional geostrophic transport.

[41] Time-series of the overturning at high latitudes is strongly correlated with the coherent, bottom pressure changes along the continental slope. In particular, a high-latitude increase in overturning is associated with a decrease in the bottom pressure along the shelf, as well as an increase in the bottom pressure along the continental slope at depths between 1000 m and 3000 m, for the western boundary. These coherent, correlation patterns between bottom pressure and overturning are very similar to the altimetric diagnostics of *Hughes and Meredith* [2006], supporting the view that high-frequency, sea-surface height variations and low frequency, overturning changes both adjust through the same boundary wave, communication process.

[42] The sea-surface height and bottom pressure anomalies vary in the same manner on the shelf and along the upper part of the continental slope. However, in deeper waters, the baroclinic compensation leads to the sea-surface height and bottom pressure anomalies being of different sign, reflecting how the sign of the overturning changes across the main thermocline.

[43] While the isopycnic model study includes a spun up wind-driven circulation, a background overturning and realistic topography, the essential boundary wave commu-

nication process is directly analogous to that advocated by *Johnson and Marshall* [2002] for baroclinic Kelvin waves in a vertical sidewall model. Details of the correlation patterns do vary though with the smoothness of the topography and the model resolution: a rougher topography acts to attenuate the wave communication and a coarser resolution smears out the bottom pressure contrasts across the shelf and continental slope. Another difference from *Johnson and Marshall* [2002] is that there is a rapid adjustment in the southern hemisphere, suggesting a role for the barotropic mode in the adjustment process.

[44] In summary, boundary waves supported along the continental slope communicate bottom pressure changes rapidly around the edge of a basin, which in turn alters the overturning stream function. The low-frequency changes in overturning are primarily connected to the vertical contrast in bottom pressure along the western boundary with opposing signals along the shallow shelf and across the continental slope. This model-based study, together with the altimetric diagnostics of coherent sea-surface height anomalies along the continental slope, supports the view that changes in overturning can be efficiently inferred from a network of bottom-pressure measurements along the western boundary, extending from the shelf and down the continental slope. These measurements are needed at a range of latitudes in order to identify any large-scale, coherent changes in the overturning over the Atlantic basin.

[45] **Acknowledgments.** This study was supported by UK NERC RAPID grants (NER/T/S/2002/00439 and NER/T/S/2002/00485). We are grateful for constructive feedback from an anonymous referee.

References

Anderson, D. L. T., and A. E. Gill (1975), Spin up of a stratified ocean, with application to upwelling, *Deep-Sea Res.*, *22*, 583–596.

Anderson, D. L. T., and P. D. Killworth (1977), Spin up of a stratified ocean, with topography, *Deep-Sea Res.*, *24*, 709–732.

Baehr, J., J. Hirschi, J.-O. Beismann, and J. Marotzke (2004), Monitoring the meridional overturning circulation in the North Atlantic: A model-based array design study, *J. Mar. Res.*, *62*, 283–312.

Bingham, R., and C. W. Hughes (2008), Determining North Atlantic meridional transport variability from pressure on the western boundary: A model investigation, *J. Geophys. Res.*, doi:10.1029/2007JC004679, in press.

Bingham, R. J., V. Roussenov, C. W. Hughes, and R. G. Williams (2007), Meridional coherence of the North Atlantic meridional overturning circulation, *Geophys. Res. Lett.*, *34*, L23606, doi:10.1029/2007GL031731.

Blaker, A. T., B. Sinha, V. O. Ivchenko, N. C. Wells, and V. B. Zalesny (2006), Identifying the roles of the ocean and atmosphere in creating a rapid equatorial response to a Southern Ocean anomaly, *Geophys. Res. Lett.*, *33*, L06720, doi:10.1029/2005GL025474.

Bleck, R., and L. T. Smith (1990), A wind-driven isopycnic coordinate model of the North and Equatorial Atlantic Ocean. 1: Model development and supporting experiments, *J. Geophys. Res.*, *95*, 3273–3285.

Clarke, A. J., and S. Van Gorder (1994), On ENSO coastal currents and sea levels, *J. Phys. Oceanogr.*, *24*, 661–680.

Cunningham, S. A., et al. (2007), Temporal variability of the Atlantic meridional overturning circulation at 26.5N, *Science*, *317*(5840), 935–938.

Ducet, N., P.-Y. Le Traon, and G. Reverdin (2000), Global high resolution mapping of ocean circulation from TOPEX/Poseidon and ERS-1/2, *J. Geophys. Res.*, *105*, 19,477–19,498.

Enfield, D. B., and J. S. Allen (1980), On the structure and dynamics of monthly mean sea level anomalies along the Pacific coast of North and South America, *J. Phys. Oceanogr.*, *10*, 557–558.

Février, S., J. Sirven, and C. Herbaut (2007), Interaction of a coastal Kelvin wave with the mean state in the Gulf Stream separation area, *J. Phys. Oceanogr.*, *37*, 1429–1444.

Hirschi, J., and J. Marotzke (2007), Reconstructing the meridional overturning circulation from boundary densities and the zonal wind stress, *J. Phys. Oceanogr.*, *37*, 743–763.

Hughes, C. W., and M. Meredith (2006), Coherent sea-level fluctuations along the global continental slope, *Philos. Trans. R. Soc. London, Ser. A*, *364*, 885–901.

Huthnance, J. M. (1978), On coastal trapped waves: Analysis and numerical calculations by inverse iteration, *J. Phys. Oceanogr.*, *8*, 74–92.

Huthnance, J. M., L. A. Mysak, and D.-P. Wang (1986), Coastal trapped waves, baroclinic processes on continental shelves, *Coastal Estuarine Sci.*, *3*, 1–18.

Johnson, H. L., and D. P. Marshall (2002), A theory for the surface Atlantic response to thermohaline variability, *J. Phys. Oceanogr.*, *32*, 1121–1132.

Kawase, M. (1987), Establishment of deep ocean circulation driven by deep-water production, *J. Phys. Oceanogr.*, *17*, 2294–2317.

Marotzke, J. R., K. Giering, Q. Zhang, D. Stammer, C. Hill, and T. Lee (1999), Construction of the MIT ocean general circulation model and application to Atlantic heat transport sensitivity, *J. Geophys. Res.*, *104*, 29,529–29,547.

Meyers, S. D., A. Melsom, G. T. Mitchum, and J. J. O'Brien (1998), Detection of the fast Kelvin wave teleconnection due to the El Nino Southern Oscillation, *J. Geophys. Res.*, *103*, 27,655–27,663.

Mysak, L. A. (1980), Topographically trapped waves, *Ann. Rev. Fluid Mech.*, *12*, 45–76.

Roussenov, V., R. G. Williams, C. Mahaffey, and G. A. Wolff (2006), Does the transport of dissolved organic nutrients affect export production in the Atlantic Ocean?, *Global Biogeochem. Cycles*, *20*, GB3002, doi:10.1029/2005GB002510.

Wang, D.-P., and C. N. K. Mooers (1976), Coastal-trapped waves in a continuously stratified ocean, *J. Phys. Oceanogr.*, *6*, 853–863.

R. J. Bingham and C. W. Hughes, Proudman Oceanography Laboratory, 6 Brownlow Street, Liverpool L3 5DA, UK.

V. M. Roussenov and R. G. Williams, Department of Earth and Ocean Sciences, University of Liverpool, Liverpool L69 3GP, UK. (v.roussenov@liverpool.ac.uk)